

Available online at www.sciencedirect.com**SciVerse ScienceDirect**

Procedia Engineering 41 (2012) 120 – 126

**Engineering
Procedia**
www.elsevier.com/locate/procedia

International Symposium on Robotics and Intelligent Sensors 2012 (IRIS 2012)

Robust Disturbance Rejection Control of Helicopter System Using Intelligent Identification of Uncertainties

Safanah M. Raafat^a, Rini Akmeliawati^{b*}^a*IIUM, Gombak, Kuala Lumpur 50728, Malaysia; UOT, Baghdad, Iraq*^b*IIUM, Gombak, Kuala Lumpur 50728, Malaysia,*

Abstract

This paper addresses the problem of designing a robust control for a laboratory 3DOF helicopter system. Simplified and disturbance rejection robust controllers are presented for the linearized dynamical system. The robust controller is formulated as a mixed H_2/H_∞ problem. An Adaptive Neuro Fuzzy Inference System (ANFIS) is used for intelligent estimation of uncertainties. This paper is dedicated to robustly compensate for the effects of modelling uncertainties and disturbances on the helicopter system, using intelligent estimation. Further study on the design and controller implementation issues is now being developed.

© 2012 The Authors. Published by Elsevier Ltd. Selection and/or peer-review under responsibility of the Centre of Humanoid Robots and Bio-Sensor (HuRoBs), Faculty of Mechanical Engineering, Universiti Teknologi MARA.

Open access under [CC BY-NC-ND license](https://creativecommons.org/licenses/by-nc-nd/4.0/).

Keywords: *Keywords:* Adaptive Neuro Fuzzy Inference System (ANFIS); disturbance rejection robust control; linearized dynamical system; mixed H_2/H_∞ ; uncertainties; 3DOF helicopter system.

Nomenclature

G_e	the model error frequency response function
K	feedback robust controller
W_{ai}	uncertainty weighting function
W_{di}	disturbance weighting function
W_{ei}	performance weighting function
W_{ui}	control weighting function
q	the generalized coordinates
η_{di}	the disturbance

1. Introduction

Recently, there is a renewed interest in helicopter control, particularly with the increased use of rotary type unmanned aerial vehicles. The nonlinear characteristics of the system as well as high coupling among its states have made the control of such system a confronting control problem. In this study, a laboratory scale version with 3DOF is considered as a typical

* Corresponding author. Tel.: +0-000-000-0000 ; fax: +0-000-000-0000 .

E-mail address: smraafat@uotbaghdad.edu

benchmark for experimental purposes in control design. This is mainly useful for justification of control scheme during the developmental stage of full flight control law.

As the helicopter is an *under-actuated mechanical system* [1], many problems arise due to under actuation like non-linearity and non-minimum phase system properties. Moreover, there are unavoidable effects of uncertainties in the mechanical system model which may further increase the difficulties. That motivates the development of robust control of helicopter system. Many approaches were applied to a helicopter control problem. Linear Quadratic regulator (LQR) is among the most commonly used state-space controllers for helicopter system [2] [3], [4], [5]. However, due to the highly nonlinear nature of the helicopter system and the need for robustness of the design, other approaches that implement nonlinear based robust control methods have been also developed, [6], sliding control which is a likely choice [7], and multiple-surface sliding controller (MSSC) [8]. Nevertheless, the standard sliding for a helicopter might phase some difficulties due to chattering.

Recently, development and application of the H_∞ design method has gained much interest due to its promising characteristics: the ability to specify the closed-loop system's frequency response by means of requirements on the sensitivity and the complementary sensitivity, and the ability to minimize undesirable resonance in the frequency response while closing all loops from input to the output vector in an essential single design step [9].

In this paper, an intelligent robust H_2/H_∞ controller is developed using two different robust control schemes; simplified and disturbance rejection. Simulation results on a linearized helicopter system model reveal the benefits of combining intelligent system identification and robust control: significant performance improvements vs. conventional LQR and robust control have been achieved.

The paper is organized as follows; Section 2 presents the helicopter dynamics and modelling, Section 3 presents the intelligent robust control design, Section 4 discusses the results and finally, Section 5 concludes the paper.

2. Helicopter Dynamics: Description and Modelling

The laboratory scale 3DOF helicopter system [1] consists of two DC motors mounted at the two ends of a rectangular frame (helicopter frame) that drive two propellers (back and front propellers). There are two inputs voltages: one for the front motor and the other for the back motor are required to generate the necessary thrusts vectors to control the system in the three degree of freedom. The generated thrust vectors are related to rate of elevation, pitch and travel. From the definition of the Euler-Lagrange system, the dynamical model of the helicopter can be derived from the knowledge of its energy functions [1].

The following definition provides a formal formulation of mechanical system.

Definition [10] The Lagrangian equations for the helicopter mechanical system may be written as:

$$M(q_i) + C(q_i, \dot{q}_i) \dot{q}_i + G(q_i) = F_e \quad (1)$$

$$\text{where} \quad G(q_i) = \frac{du}{dq_i}(q_i) \in \mathbb{R}^n, \quad C(q, \dot{q}) = \sum_{k=1}^n \Gamma_{hjk} \dot{q}_k \quad (2)$$

and Γ_{ijk} are called the Christoffel's symbols associated with the inertia matrix $M(q)$ and are defined by:

$$\Gamma_{hjk} = \frac{1}{2} \left(\frac{\partial M_{hj}}{\partial q_k} + \frac{\partial M_{hk}}{\partial q_j} - \frac{\partial M_{kj}}{\partial q_h} \right) \quad (3)$$

For the 3DOF helicopter, the generalized coordinates, q are defined in terms of the elevation, ϵ , pitch, p , and travel, λ angles:

$$q = [\epsilon(t), p(t), \lambda(t)]^T \quad (4)$$

The external forces F_e comprises of the force on elevation, F_ϵ , force on the pitch, F_p , and the force on the travel angles, F_λ . The thrust forces acting on the elevation, pitch, and travel axes from the front and back motors are defined and made relative to the quiescent voltage [1].

Consider the state variable vector $x := (q, \dot{q})^T$ and write the linearized model in state space representation:

$$\frac{d}{dt}x = A_m x + B_m u$$

and

$$y = C_m x + D_m u$$

The state vector for the 3- DOF Helicopter is defined

$$x = \left[\varepsilon_i, p, \lambda, \frac{d}{dt}\varepsilon_i, \frac{d}{dt}p, \frac{d}{dt}\lambda \right]^T \quad (6)$$

And the output vector is

$$y = [\varepsilon_i, p, \lambda]^T \quad (7)$$

The corresponding helicopter state space matrices are [1]

$$A_m = \begin{bmatrix} 0_{3 \times 3} & I_{3 \times 3} \\ 0_{2 \times 3} & 0_{2 \times 3} \\ 0 & -A_{6,2} & 0_{1 \times 4} \end{bmatrix}, B_m = \begin{bmatrix} 0_{3 \times 1} & 0_{3 \times 1} \\ B_{4,1} & B_{4,2} \\ B_{5,1} & B_{5,2} \\ 0 & 0 \end{bmatrix}, C_m = \begin{bmatrix} 1 & 0 & 0_{1 \times 4} \\ 0 & 1 & 0_{1 \times 4} \\ 0_{1 \times 2} & 1 & 0_{1 \times 3} \end{bmatrix}, D_m = 0_{3,2} \quad (8)$$

where

$$A_{6,2} = \frac{(L_w m_w - 2L_a m_f)g}{m_w L_w^2 + 2m_f L_h^2 + 2m_f L_a^2}, \quad B_{4,1} = B_{4,2} = \frac{L_a K_f}{2m_f L_a^2 + m_w L_w^2}, \quad B_{5,1} = -B_{5,2} = \frac{1}{2} \frac{K_f}{m_f L_h} \quad (9)$$

And for the given parameters in Table 1 [1], the numerical values of (9) are: $A_{6,2} = -1.2304$, $B_{4,1} = B_{4,2} = 0.0858$, $B_{5,1} = 0.5810$ and $B_{5,2} = -0.5810$.

Table 1. The main parameters description of the 3DOF helicopter[1]

Symbol	Description	Value	Units
K_f	Propeller force- thrust Constant	0.1188	N/V
m_w	Mass of the counterweight	1.87	Kg
m_f	Mass of front propeller Assembly	0.713	Kg
L_a	Distance between travel axis to helicopter body	0.660	m
L_h	Distance between pitch axis to each motor	0.178	m
L_w	Distance between travel axis to the counterweight	0.470	m
g	Gravitational constant	9.81	m/s ²

3. Robust Control Design for the Helicopter System

For robust controller design, the helicopter system is described by a nominal model and a bounded uncertainty. These uncertainties introduce the effect of errors through frequency dependent weighting functions [11]. The aim of these weights is to reproduce the effect of component and modelling errors in the description of the actual plant. The better this relationship is known, the more efficient the unstructured uncertainty weights will be in synthesizing a robust controller that will accumulate performance requirements in the actual environment of the plant.

3.1. Simplified H_∞ Robust Controller Design

Figure (1) shows the constructed closed loop system, where W_{u1}, W_{u2} are control weighting functions and W_{e1}, W_{e2}, W_{e3} are performance weighting functions. The selection of the weighting functions W_{e1} and W_{u1} follows that in [11],[12], while the selection of the uncertainty weighting functions W_{a1}, W_{a2} is accomplished as will be discussed in Section 3.2.

In order to satisfy some objectives; robust stability, robust performance, faster tracking and reduced effects of uncertainties and measurements errors, the robust controller is formulated as a mixed H_2/H_∞ problem. The prescribed specifications are translated into the following criterion [13]:

$$\text{Minimize } \alpha \|T_\infty\|_\infty^2 + \beta \|T_2\|_2^2 \quad (10)$$

while maintaining the H_∞ of the closed loop transfer function T_∞ from ω_i to $z_\infty < \gamma_0$ and maintaining the H_2 of the closed loop transfer function T_2 from ω_i to $z_2 < \nu_0$, where $\gamma_0 > 0$ and $\nu_0 > 0$ are some prescribed value. Moreover, the closed loop poles will be placed in the Linear Matrix Inequalities (LMI) open left hand plan region.

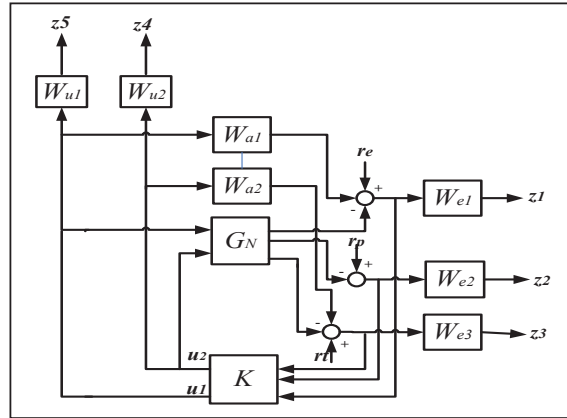


Fig. 1. The entire-connection of the robustly-controlled system.

3.2. Intelligent Estimation of Uncertainty Bounds for H_∞ Robust Controller Design

The most common problem with robust controller design is that it results in a conservative control action since it is based on the worst case assumptions [11]. In order to overcome this limitation an intelligent estimation of uncertainty bounds is developed in [14], using Adaptive Neuro Fuzzy Inference System (ANFIS).

The main purpose of the intelligent uncertainty identification is to calculate approximately the upper magnitude bound of the model error frequency response function $G_e(j\omega)$ [13]:

$$|G_e(j\omega)| = |G_r(j\omega) - G_N(j\omega)| = \frac{|E(j\omega)|}{|U(j\omega)|} \quad (11)$$

where $G_r(j\omega)$ is the measured frequency response function of the actual system, $G_N(j\omega)$ is the frequency response function of the nominal linear model of the system, $E(j\omega)$ is the Fast Fourier Transform (FFT) of prediction error $e(t)$ and $U(j\omega)$ is the FFT of $u(t)$. Note that plant uncertainties and non-deterministic effects give rise to frequency dependent intervals associated with $|G_e(j\omega)|$.

3.3. Disturbance Rejection Scheme for Robust Controller Design

In order to compensate for the effects of interaction between the different axes in the robust controller design, the entire connection configuration of (Figure 1) is considered with additional disturbance weighting functions. The main idea is to shape the closed- loop Sensitivity $S = (1 + G_N K)^{-1}$ and complementary functions $T = 1 - S = (1 + G_N K)^{-1} G_N K$ with weighting functions W_{ei} , W_{ai} , W_{ui} and W_{di} to achieve robust stability, model error compensation, disturbance rejection, and noise attenuation, and to make the closed- loop response close to a target reference r_i . The weighting function W_{d1} reflects the frequency contents of the disturbing effect of input u_2 and the weighting function W_{d2} reflects the frequency contents of the disturbing effect of input u_1 . Applying a similar approach to the estimation of uncertainty using ANFIS (in Section 3.2), and using experimentally collected data, intelligent disturbance weighting functions had been estimated in order to accurately attenuate the effect of crosstalk disturbance in specific frequency range on the control signal. In this case, the regulated outputs are chosen as $e_i = r_i - y_i$, the deviation from target response, the weighted error $z_{1,2,3}$, and the weighted control $z_{4,5}$. Detailed description can be found in [15].

In order to simplify the development of the entire connection, the control input voltage to the plant is arranged to include

both the control signal voltage $u_{1,2}$ and the weighted disturbance effect $W_{di}\eta_{di}$, where η_{d1} and η_{d2} are the disturbances. Therefore, it will be formulated as

$$u_{di} = u_i + W_{di}\eta_{di} \quad (12)$$

4. Simulation Results

The application of robust control synthesis for the 3DOF helicopter is presented in this section. Based on the state space model described by (5), the robust controller is designed to satisfy (10). However, the obtained robust controller is of high order, 13, and model order reduction is necessarily applied to obtain the suitable control action of order 8. For a tracking and regulation control problem, the system states are augmented with two extra integral states vector to improve the tracking performance [1], providing that the sensitivity of the robustly controlled is satisfied.

Figure (2) shows a comparison of elevation responses to a square input signal between two robust controllers as well as Quanser LQR controller. It is shown that the designed H_∞ robust controller can achieve better transient performance (i.e. settling time, overshoot and steady state error) compared with that of LQR. Specifically, the robust controller with intelligently estimated uncertainty weighting functions can provide more accurate results. Similarly, Figures (3) and (4) presents the comparison results of pitch and travel responses using the robust controller and the Quanser LQR controlled system. Figures (5) and (6) show the controlled signals of the front and back motors. Reduced control signals are achieved by the robust controllers.

Figure (7) shows the elevation responses of the three developed robust controllers. The robust controller with disturbance rejection configuration improves the transient response of the controlled system, as compared with the other two robust controllers. The same can be observed in Figures (8) and (9). Though, the overshoot of the pitch response has increased. These changes can be related to the increased control signals of the front and back motors due to the inclusion of the coupling effects, as shown in Figures (10) and (11).

It was observed from the experimentally obtained data and from the estimated disturbance weighting functions that most of the coupling effects are related to the elevation and travel states. Nevertheless, the applied experimental treatment can efficiently compensate for the coupling effects within limited range of perturbations.

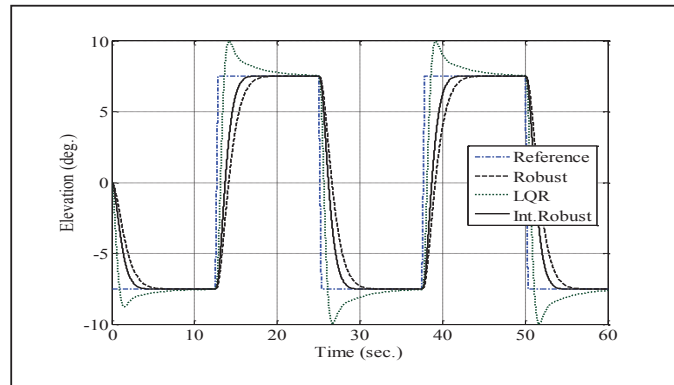


Fig. 2. Elevation responses of the robust control, intelligent robust control, and Quanser LQR with square input (by simulation).

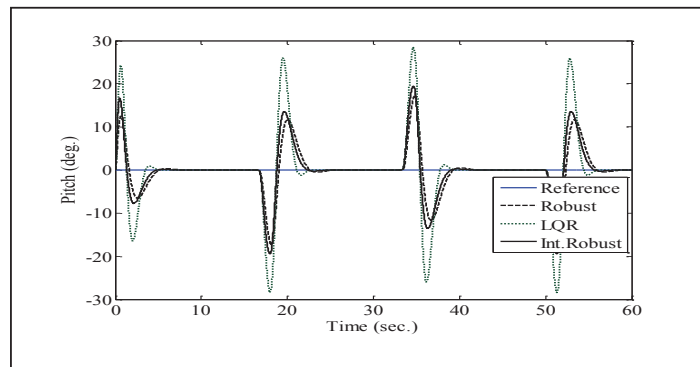


Fig. 3. Pitch responses of the robust control, intelligent robust control, and Quanser LQR (by simulation).

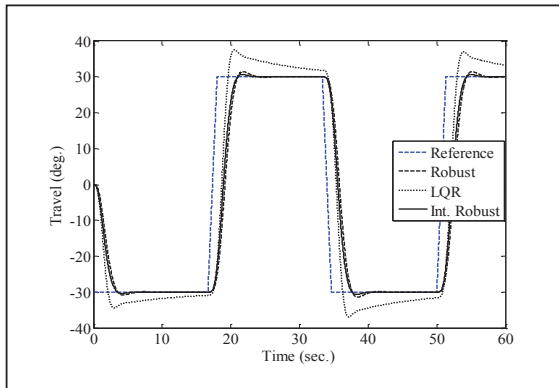


Fig. 4. Travel responses of the robust control, intelligent robust control, and Quanser LQR with square input (by simulation).

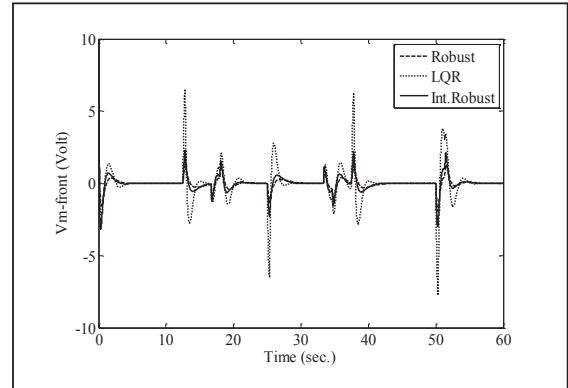


Fig. 5. Front motor control signals of the robust control, intelligent robust control, and Quanser LQR with square input (by simulation).

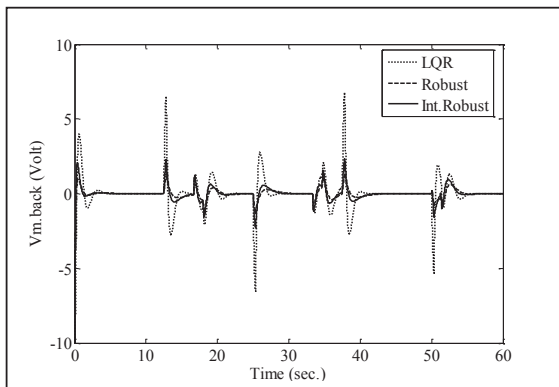


Fig. 6. Back motor control signals of the robust control, intelligent robust control, and Quanser LQR with square input (by simulation).

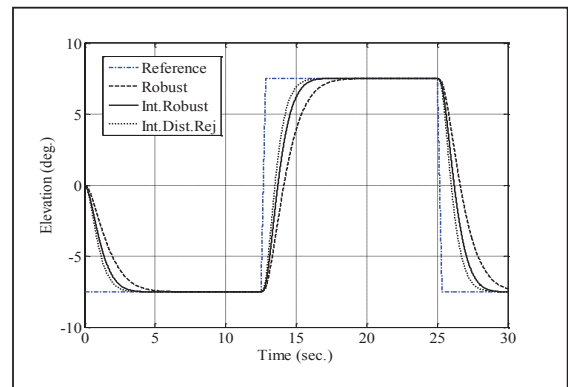


Fig. 7. Elevation response signals of the intelligent-disturbance rejection robust control, intelligent robust control, and robust control with square input (by simulation).

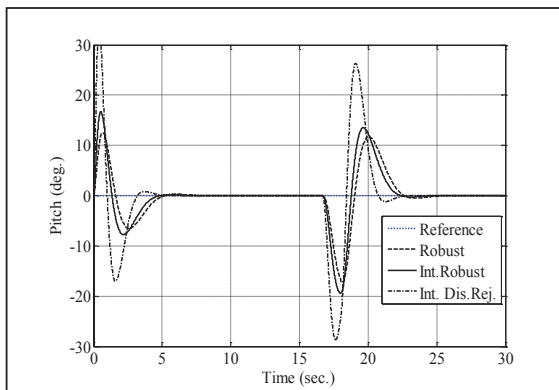


Fig. 8. Pitch response signals of the intelligent-disturbance rejection robust control, intelligent robust control, and robust control with square input (by simulation).

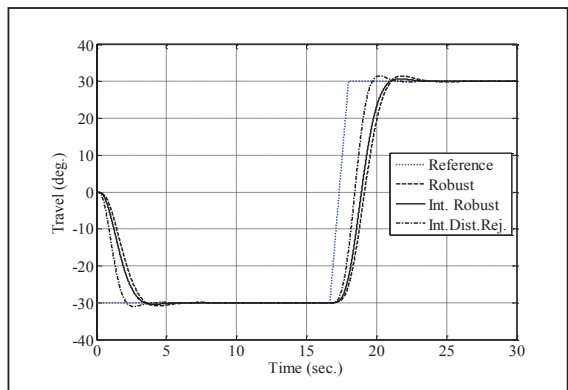


Fig. 9. Travel response signals of the intelligent-disturbance rejection robust control, intelligent robust control, and robust control with square input (by simulation).

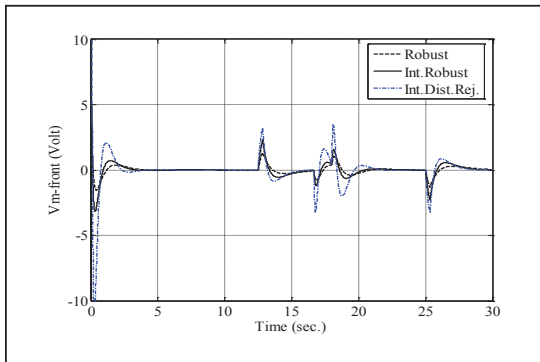


Fig.10. Front motor control signals of the intelligent-disturbance rejection robust control, intelligent robust control, and robust control with square input (by simulation).

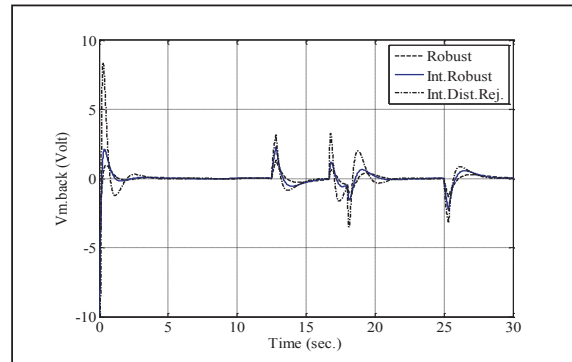


Fig.11. Back motor control signals of the intelligent-disturbance rejection robust control, intelligent robust control, and robust control with square input (by simulation).

5. Conclusion

In this paper, simplified robust and robust disturbance rejection controllers have been developed for the linear dynamic model of a 3DOF helicopter. The modelling uncertainties and disturbance effects were estimated using ANFIS. Two H_2/H_∞ robust controllers were synthesized using intelligently estimated weighting functions. Simulation results and comparison with a conventional LQR controller demonstrate that the performance of the closed loop system with the designed robust controllers had improved considerably and the control effort was reduced. The accuracy and simplicity of the proposed approach encourage its applications for other dynamical systems, such as vehicles and robots.

References

- [1] Quanser Inc. (2006). *3DOF Helicopter system, product information*, available <http://www.quanser.com>, Ontario (Canada).
- [2] Brian L. Stevens and Frank L. Lewis, (1992). *Aircraft control and simulation*, John Wiley & Sons, Inc.
- [3] Alvis, W., Castillo, C., Castillo-Effen, M., Moreno, W., Valavanis, K. P. (2007). A Tutorial Approach to Small Unmanned Helicopter Controller Design for Nonaggressive Flights. Kimon P. Valavanis (ed.), *Advances in Unmanned Aerial Vehicles*, 119–170. © 2007 Springer. Netherlands.
- [4] Hao, L., Yao, Y., Geng, L., and Yisheng, Z. (2010). Robust LAR Attitude control of 3DOF Helicopter, *proceeding of the 29th Chinese control conference*, July 29–31, Benjing, China.
- [5] Tijani, I.B., Akmeliawati, R., Legowo, A. and Muthalif, A.G.A. (2011). Optimized LQR controller synthesis for 3DOF helicopter using multi-objective differential evaluation (mode). *Computational Intelligence in Robust Control*. Ch.2. IIUM. Malaysia. To be published.
- [6] Yao, Y. and YiSheng, Z. (2008). Robust Tracking Control for a 3DOF Helicopter with Multi-operation Points. *Proceedings of the 27th Chinese Control Conference*. July 16–18, 2008, Kunming, Yunnan, China, 733–737.
- [7] Starkov, K. K., Aguilar, L. T. and Orlov, Y. (2008). Sliding mode control synthesis of a 3-DOF helicopter prototype using position feedback. *IEEE. Variable Structure Systems, 2008. VSS '08. International Workshop on*. 8–10 June 2008, 233 – 237.
- [8] Hamood, M. A., Akmeliawati, R. and Legowo, A. (2011). Multiple-surface sliding mode control for 3DOF helicopter. *2011 4th International Conference on Mechatronics (ICOM)*, 17–19 May 2011, Kuala Lumpur, Malaysia.
- [9] Colgren, R.D. (2004). *Applications of robust control to nonlinear systems*. American Institute of Aeronautics and Astronautics, Inc.
- [10] Lozano, R., Borgilato, B., Egeland, O., and Maschkem B. (2000). *Dissipative Systems Analysis and Control*. Springer Verlege, London.
- [11] Zhou, K. and Doyle, J.C. *Essentials of Robust Control*, Prentice-Hall, Inc. 1998.
- [12] Akmeliawati, R., Raafat, S. M. and Wahyudi, Improved Intelligent Identification of Uncertainty Bounds; Design, Model Validation and Stability Analysis, *International Journal of Modelling, Identification, and Control*, 15(3), 2012, 173–184.
- [13] Balas, G., Chiang, R., Packard, A. and Safonov. *Robust Control ToolboxTM3* user's guide, 2010, MathWorks.
- [14] Raafat, S. M., Akmeliawati, R. and Wahyudi, Intelligent Robust Control Design of a Precise Positioning System, *International Journal of Control, Automation and Systems*, 8(5), Oct. 2010.
- [15] Raafat, S. M., Akmeliawati, R. and Wahyudi, Intelligent Disturbance Rejection for Robust Tracking Performance of X-Y Positioning System, *Proc. Of the IEEE Int. Conf. on Mechatronics and Automation*, Xi'an China, August 4–7, 2010, 252–257.